Langmuir

Article

pubs.acs.org/Langmuir

Novel Cellulose Polyampholyte–Gold Nanoparticle-Based Colorimetric Competition Assay for the Detection of Cysteine and Mercury(II)

Jun You,[†] Haoze Hu,[†] Jinping Zhou,*[,†,‡] Lina Zhang,[†] Yaping Zhang,[§] and Tetsuo Kondo[‡]

[†]Department of Chemistry, Wuhan University, Wuhan 430072, China

[‡]Graduate School of Bioresource and Bioenvironmental Sciences, Kyushu University, 6-10-1, Hakozaki, Higashi-ku, Fukuoka 812-8581, Japan

[§]State Key Laboratory Cultivation Base for Nonmetal Composites and Functional Materials, Southwest University of Science and Technology, Mianyang, 621010, China

Supporting Information

ABSTRACT: We provide a highly sensitive and selective assay to detect cysteine (Cys) and Hg^{2+} in aqueous solutions using Au nanoparticles (NPs) stabilized by carboxylethyl quaternized cellulose (CEQC). This method is based on the thiophilicity of Hg^{2+} and Au NPs as well as the unique optical properties of CEQC-stabilized Au NPs. CEQC chains are good stabilizing agents for Au NPs even in a high-salt solution. The addition of Cys results in the aggregation of CEQC-stabilized Au NPs, which induces the visible color change and obvious redshift in UV–visible absorption spectra. On the other hand, Hg^{2+} is more apt to interact with thiols than Au NPs; thus, it can remove the Cys and trigger Au NP aggregate redispersion again. By taking advantage of this mechanism, a novel off–on colorimetric sensor has been established for Cys and Hg^{2+} detection. This new assay could selectively detect Cys and Hg^{2+} with the detection limits as low as 20 and 40 nM in aqueous solutions, respectively.

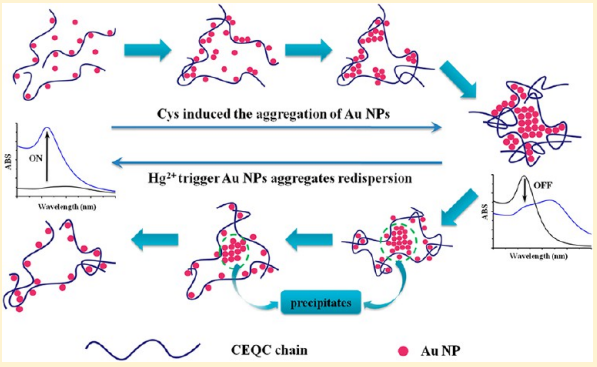

INTRODUCTION

As an essential amino acid, cysteine (Cys) plays a crucial biological role in the human body including protein synthesis, detoxification, and metabolism.[1] Particularly, Cys has been proven to act as the physiological regulator in various diseases such as heart disease, rheumatoid arthritis, and AIDS.[2,3] On the other hand, Hg^{2+} ions are toxic heavy metal pollutants that widely exist in water, soil, and even food. It can cause serious health problems such as anemia, liver and kidney damage, diabetes, and heart failure.[4] It is estimated that the total mercury released into the environment reaches to ~7500 tons per year.[5] The detection of Cys and Hg^{2+} is important and has become an increasing demand in recent years. A great effort has been exerted to detect Cys and Hg^{2+} using various detection techniques, including optical spectroscopy,[6−10] electrochemical methods,[11,12] high-performance liquid chromatography,[13,14] inductively coupled plasma mass spectrometry,[14,15] and so forth.[14,15] However, most of these techniques require expensive instrumentation and complicated sample preparation in certain cases, which make them inappropriate for point-of-use applications. To overcome these drawbacks, a variety of colorimetric sensors based on Au nanoparticles (NPs) have been attempted for the simple, rapid detection of Cys and Hg^{2+}.[16−19]

The aggregation of spherical Au NPs can induce a rapid visible color change from red to blue due to the coupling of interparticle surface plasmon.[20−22] The color change provides a practical platform for the colorimetric detection of analyte that can induce the Au NP aggregation or redispersion. More importantly, the extinction coefficients of Au NPs are over 1000 times larger than those of organic dyes,[23] which makes them very suitable for applications in colorimetric sensing systems.[24] For example, Liu et al. provided a highly sensitive and selective assay to detect Hg^{2+} in aqueous solutions using quaternary ammonium group-terminated thiols modified Au NPs.[25] Lee et al. developed a highly sensitive and selective colorimetric detection for Cys based upon oligonucleotide-functionalized Au NPs probes that contain strategically placed thymidine–thymidine (T–T) mismatches complexed with Hg^{2+}.[19] In most cases, Au NPs are modified with oligonucleotide- or thiol-containing organic molecules to indicate color or light intensity change. These assays own some advantages, but they are still cost- or pollution-consuming.[26] Therefore, it is interesting

Received: December 22, 2012
Revised: March 25, 2013
Published: March 25, 2013

and necessary to develop a facile, low cost, rapid, and eco-friendly method for Cys and Hg^{2+} detection.

Cellulose is one of the most common polysaccharides and is considered an almost inexhaustible polymeric raw material with fascinating structure and properties.[27] However, cellulose cannot be dissolved in conventional solvents, which limited its further application. In previous work, a water-soluble quaternized cellulose (QC) was homogeneously synthesized from cellulose directly in alkali/urea aqueous solutions and had been studied as gene[28,29] and protein carriers,[30] thermoirreversible gels,[31] and so forth. In this work, a novel cellulose polyampholyte (CEQC, Scheme 1) was further homogeneously synthesized from QC, which displayed good salt-resistance and pH-sensibility. A label-free colorimetric assay is developed for sensing both Cys and Hg^{2+} in aqueous solutions based on CEQC-stabilized Au NPs. Au−CEQC solutions are shown to act as an off−on UV absorption switch. Cys turns off the switch by inducing the formation of Au NP aggregates, whereas Hg^{2+} turns on the UV−visible (UV−vis) signal because it competitively binds to Cys.

Scheme 1. Chemical Structure of CEQC

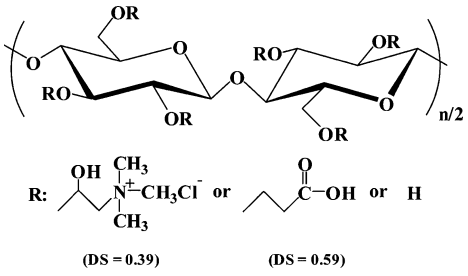

EXPERIMENTAL SECTION

Materials. The cellulose (cotton linter pulp) was supplied by Hubei Chemical Fiber Group Ltd. (Xiangyang, China), and the viscosity-average molecular weight (M_η) was determined by viscometry in cadoxen to be 12.5×10^4 g/mol. Amino acids were purchased from Shanghai Ruji Biology Technology Co., Ltd. Other chemical regents ($HAuCl_4$, $NaBH_4$, etc.) were purchased from Sinopharm Chemical Reagent Co., Ltd. and were used without further purification. Deionized water (Millipore) was used for all experiments.

Preparation of CEQC. QC was homogeneously synthesized in LiOH/urea aqueous solution according to previous work.[28] The substitution degree (DS) of the quaternary ammonium was determined to be 0.39 by using elemental analysis. QC was further modified with acrylamide under alkaline conditions. Then, CEQC was obtained by further hydrolysis of the acrylamide-modified QC.[32] The DS of carboxyl groups was determined by elementary analysis and NMR to be 0.59. The isoelectric point (IEP) was determined to be 3.8 through zeta potential and viscosimetry measurements.

Preparation of Au NPs. Au NPs were synthesized by directly reducing $AuCl_4^-$ ions in CEQC aqueous solutions using $NaBH_4$ as the reducing agent. CEQC cannot be dissolved in pure water for its antipolyelectrolyte effect; thus, 0.1 M $NaNO_3$(aq) was selected as the solvent. Typically, 1 mg/mL CEQC solution was prepared by dissolving 10 mg of CEQC in 10 mL of $NaNO_3$(aq) and was further stirred for 24 h at room temperature. Then, 1 mL of $HAuCl_4$ (2.428×10^{-2} M) solution was added into 10 mL of CEQC solution (1 mg/mL) in a reaction vessel, followed by constant stirring for 10 min. At last, 0.5 mL of $NaBH_4$ (0.1 M) solution was added immediately with vigorous stirring. The color of the solution changed from faint yellow to deep red in a few seconds. The obtained concentration of Au NPs in CEQC(aq) was 2.0×10^{-6} M.

Detection of Cys Using Au−CEQC Solutions. First, 10 mL of Au−CEQC solution was diluted to 100 mL with 0.1 M $NaNO_3$(aq). Then, 30 μL of Cys solution with various concentrations were pipetted into the test tubes that contained 3 mL of Au−CEQC(aq) (the final Cys concentration ranged from 100 nM to 10 μM), and the corresponding UV−vis spectra were recorded. The selectivity for Cys was confirmed by adding other amino acid stock solutions to the final concentration of 100 μM instead of Cys.

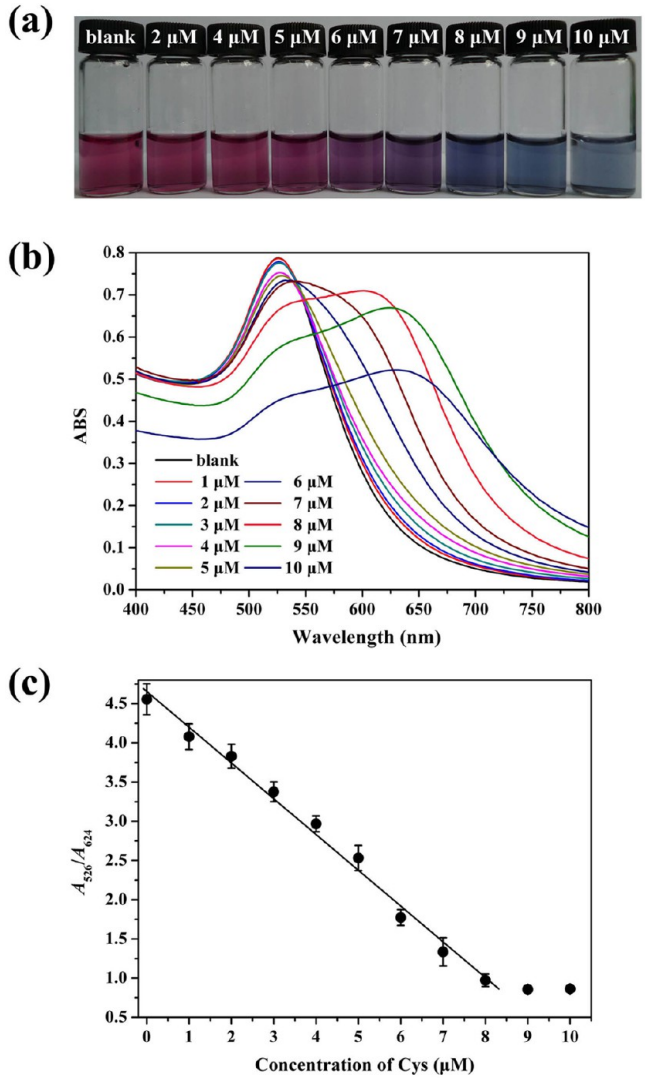

Figure 1. Colorimetric detection of Cys by Au−CEQC solutions: (a) color change of the solutions with increasing Cys concentration; (b) UV−vis spectra of the solution response for the Cys concentration; (c) plots of A_{526}/A_{624} versus the Cys concentration.

Detection of Hg^{2+} Using Au−CEQC/Cys Complex. A 30 μL amount of Cys (5 mg/mL) solution was added to 10 mL of Au−CEQC(aq) with vigorous stirring, and then, the mixed solution was diluted to 90 mL with $NaNO_3$(aq). After that, the pH value of the mixed solution was adjusted to 11.2 by adding 10 mL of 0.1 M NaOH(aq) (the final Cys concentration was 12.4 μM). At last, 50 μL of Hg^{2+} ions was pipetted into the test tubes that contained 3 mL of the above mixed solution, and the corresponding UV−vis spectra were recorded. The selectivity for Hg^{2+} was confirmed by adding other metal ions to the final concentration of 24 μM instead of Hg^{2+}.

The limits of detection (LODs) for Cys and Hg^{2+} are calculated by $3S_0/S$, where 3 is the factor at the 99% confidence level, S_0 is the standard deviation of the blank measurements (n = 12), and S is the slope of the calibration curve.[16]

Characterization. UV−vis spectra were performed on a UV−vis spectrophotometer (UV-6, Mapada, China) using quartz cuvettes with an optical path of 1 cm. Transmission electron microscopy (TEM) images were observed on a JEM-2100 (HR) electron microscope,

dx.doi.org/10.1021/la3050913 | Langmuir 2013, 29, 5085−5092

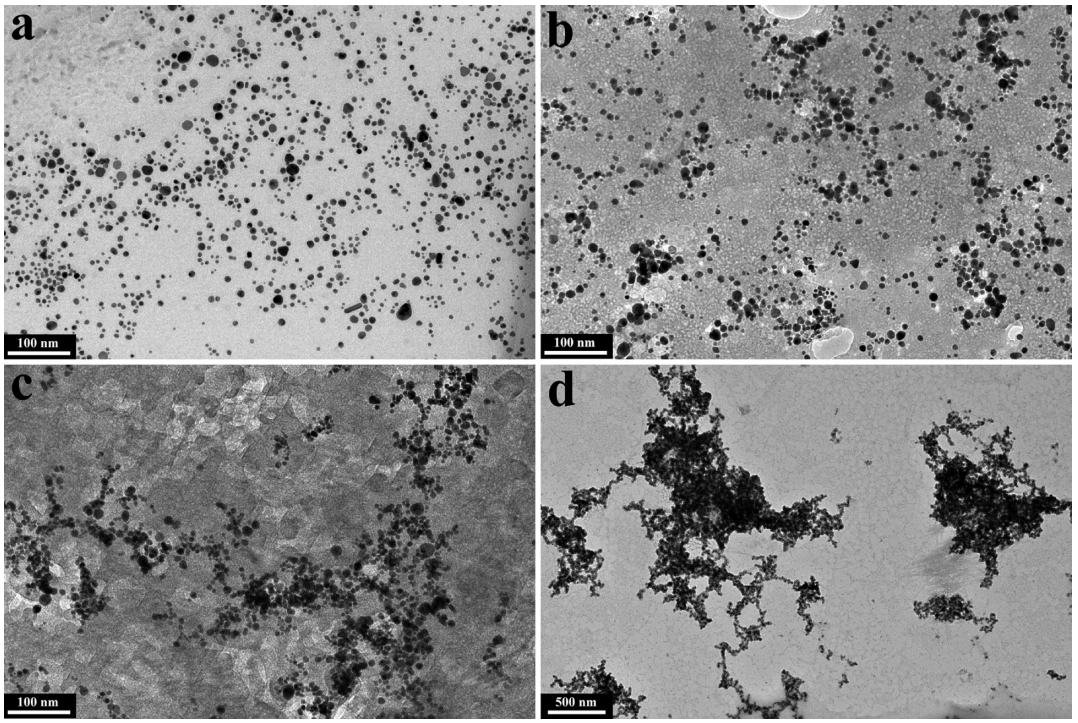

Figure 2. TEM images of CEQC-stabilized Au NPs in the (a) absence and presence of (b) 4 μM, (c) 7 μM, and (d) 8 μM Cys.

Scheme 2. Schematic Illustration for Off−On Colorimetric Detection of Cys and Hg^{2+} Ions by Au−CEQC Solutions

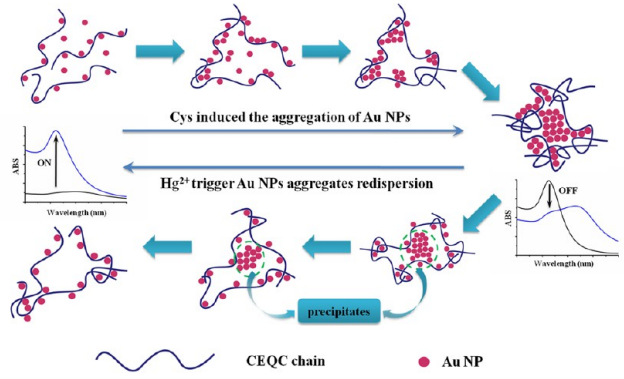

using an accelerating voltage of 200 kV. Dynamic light scattering (DLS) measurements were performed on an ALV/DLS/SLS-5000E light-scattering goniometer (ALV/CGS-8F, ALV, Germany) with vertically polarized incident light of wavelength 632.8 nm from a He−Ne laser equipped with an ALV/LSE-5003 light-scattering electronics and multiple tau digital correlator.

RESULTS AND DISCUSSION

Sensitivity of Au−CEQC to Cys. Au NPs were synthesized by directly reducing $AuCl_4^-$ ions in CEQC aqueous solution using $NaBH_4$ as the reducing agent. The obtained Au−CEQC solutions are very stable due to the existence of strong hydrogen bonding and electrostatic interactions between the Au NPs and the CEQC chains.[33,34] The prepared Au NPs displayed excellent salt-resistance in $NaNO_3$(aq) thanks to the amphoteric stabilizing agent. The UV−vis spectra of the solutions hardly changed as the $NaNO_3$ concentration increased from 0.1 to 3 M (Figure S1, Supporting Information). In order to evaluate the sensitivity of the colorimetric sensor, various concentrations of Cys solutions were added into the Au−CEQC solutions. Figure 1 shows the color of Au−CEQC solutions and their corresponding UV−vis spectra with the addition of Cys. A typical UV−vis spectrum with a Au plasmon band at approximately 526 nm was observed for the as-prepared red Au−CEQC solution. The sharp peak suggested a narrow size distribution of Au NPs. When Cys solution was added, the color of the Au−CEQC solution changed from red to purple and eventually turned to blue (Figure 1a). Meanwhile, as shown in Figure 1b, the UV−vis spectra exhibited a redshift with decreasing absorbance, whereas the signal at 624 nm was greatly enhanced. The results contributed to the fact that the aggregates of Au NPs were rapidly formed when Cys was added, producing the color change and weak absorption signals.[21,22,35] In the other words, Cys turned off the absorption signal at 526 nm. Moreover, the absorption of the solution at 624 and 520 nm corresponded to the amount of dispersed and aggregated Au NPs, respectively. Thus, the ratio between A_{526} and A_{624} (A_{526}/A_{624}) decreased linearly with an increase of Cys concentration from 0 to 8 μM, indicating an increase of the aggregation due to the continuing binding of Cys to the Au NPs (Figure 1c). With a further increase of the Cys concentration to 10 μM, the ratio (A_{526}/A_{624}) changed barely, and the solution color receded gradually due to the precipitation of Au NPs.[21,36] The LOD for Cys is approximately 20 nM (S_0 = 0.003, S = 0.459), and the sensitivity of the assay could be enhanced by reducing the concentration of Au NPs (Figure S2, Supporting Information).

Interestingly, the colorimetric sensing process was significant affected by the pH of Au−CEQC solution. As shown in Figure S3 (Supporting Information), the Au−CEQC solution displayed more sensitive detection for Cys at a relative lower pH. Sun et al. also reported that Cys (c = 0.1 mM) induced the aggregation of Au nanorods at pH below 5.0 while remaining unassembled at pH above 5.0.[37] In the present work, a relative lower concentration of Cys (c = 10 μM) was sufficient to induce the aggregation of Au NPs, presumably due to the electrostatic interaction between Cys

dx.doi.org/10.1021/la3050913 | Langmuir 2013, 29, 5085−5092

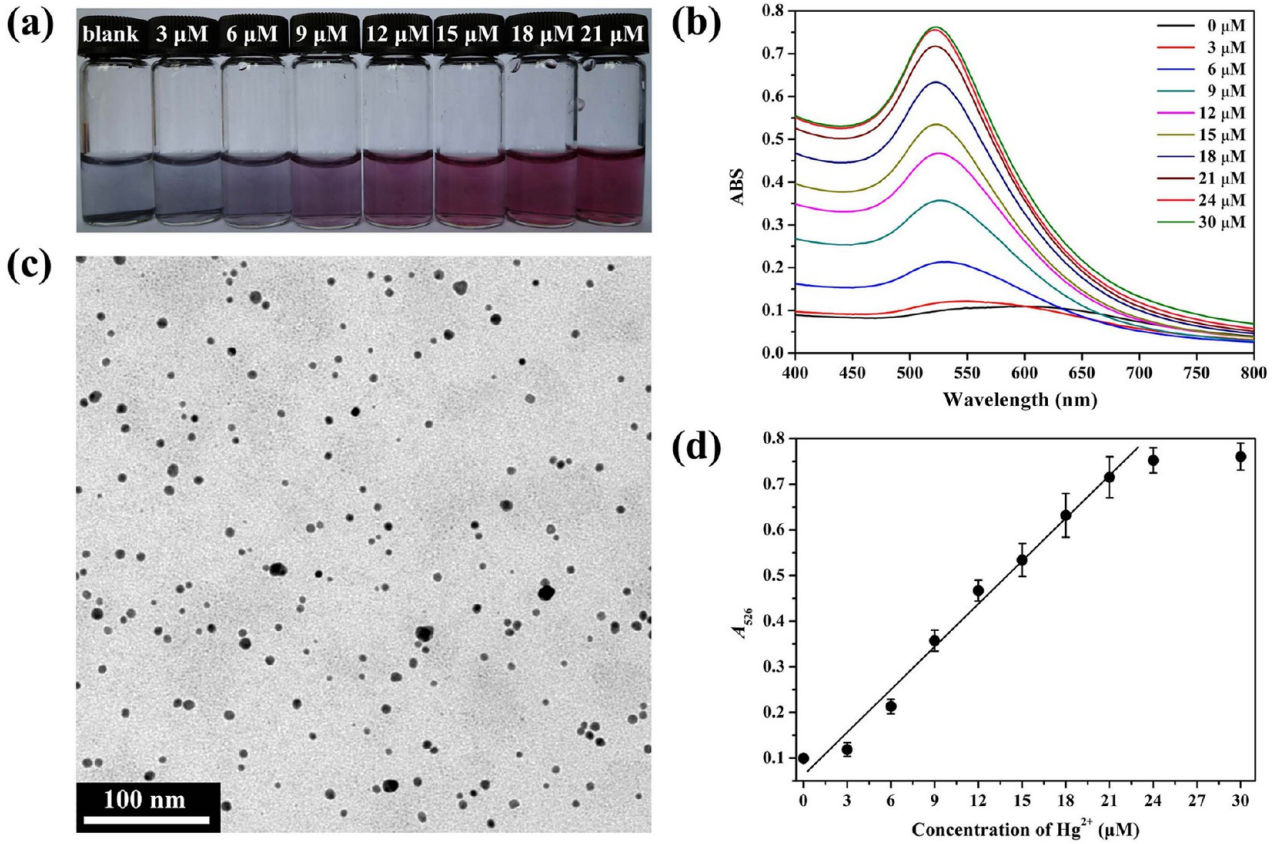

Figure 3. Colorimetric detection of Hg^{2+} by Au−CEQC/Cys systems: (a) color change of the solution with an increase of the Hg^{2+} concentration from left to right; (b) UV−vis spectra of the solutions response for the Hg^{2+} concentration; (c) TEM image of the redispersed Au NPs obtained after addition of 24 μM Hg^{2+}; (d) plots of A_{526} versus the concentration of Hg^{2+}.

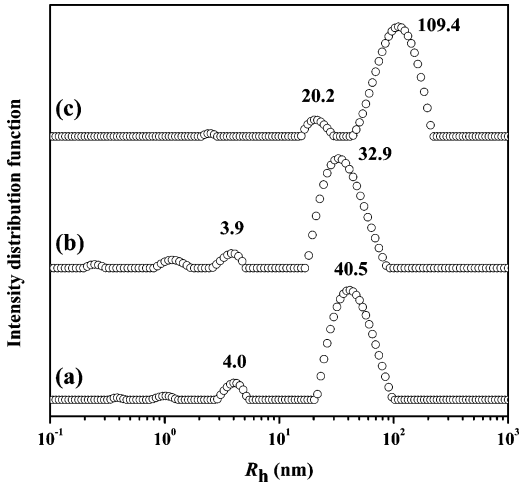

Figure 4. Corresponding hydrodynamic radius (R_h) distributions of the as-prepared Au−CEQC solutions ((a) pH = 5.2; (b) pH = 11.2) and (c) the redispersed solutions obtained by adding 24 μM Hg^{2+} to the Au−CEQC/Cys conjugate solutions.

and CEQC. Moreover, this colorimetric sensing process was ionic strength-insensitive as shown in Figure S4 (Supporting Information), due to the excellent salt-resistance of CEQC-stabilized Au NPs as we discussed previously.

Cys Induced the Aggregation of Au NPs. Direct evidence for the aggregation of Au NPs induced by Cys was supported by TEM measurement. As shown in Figure 2a, Au NPs were well dispersed in the absence of Cys due to the well protection of the stabilizing agent (CEQC). By counting more than 300 of the Au NPs in the TEM images, the statistical results showed that the mean diameter (d) and standard deviation (SD) of the Au NPs were 7.9 and 2.3 nm, respectively (Figure S5a, Supporting Information). When a small amount of Cys (4 μM) was added, the TEM image clearly showed a slight aggregation of Au NPs (Figure 2b). As expected from the UV−vis spectra, the size of the aggregates increased gradually with an increase of the Cys concentration. Finally, huge and three-dimensional random Au NPs aggregates were observed as the Cys concentration increased to 8 μM (Figure 2d). As shown in Figure S6 (Supporting Information), an obvious polymer coating even formed on the particle surface, indicating that CEQC chains aggregated with Au NPs together. The aggregation process could be explained as shown in Scheme 2. Cys was apt to bind to the Au NPs by its thiol (−SH) group, which was confirmed by many reports.[38,39] On the other hand, in the acidic environment, the carboxyl and amino groups of Cys are ionized to form a zwitterionic structure.[40,41] Thus, after Cys interacts with surface of Au NPs through its thiol group, it still has two free charged groups to interact with other Cys or CEQC chains by electrostatic interactions. In other words, Cys played a role as a cross-linking agent that made the Au NPs and CEQC chains close to each other, and finally, aggregates (even precipitates) of Au NPs and CEQC formed together.

Moreover, we also attempt to use this method to detect other thiol-containing biomolecules, such as dithiothreitol (DTT), glutathione (GSH), and bovine serum albumin (BSA). Figure S7 (Supporting Information) shows the absorbance profiles of this

dx.doi.org/10.1021/la3050913 | Langmuir 2013, 29, 5085−5092

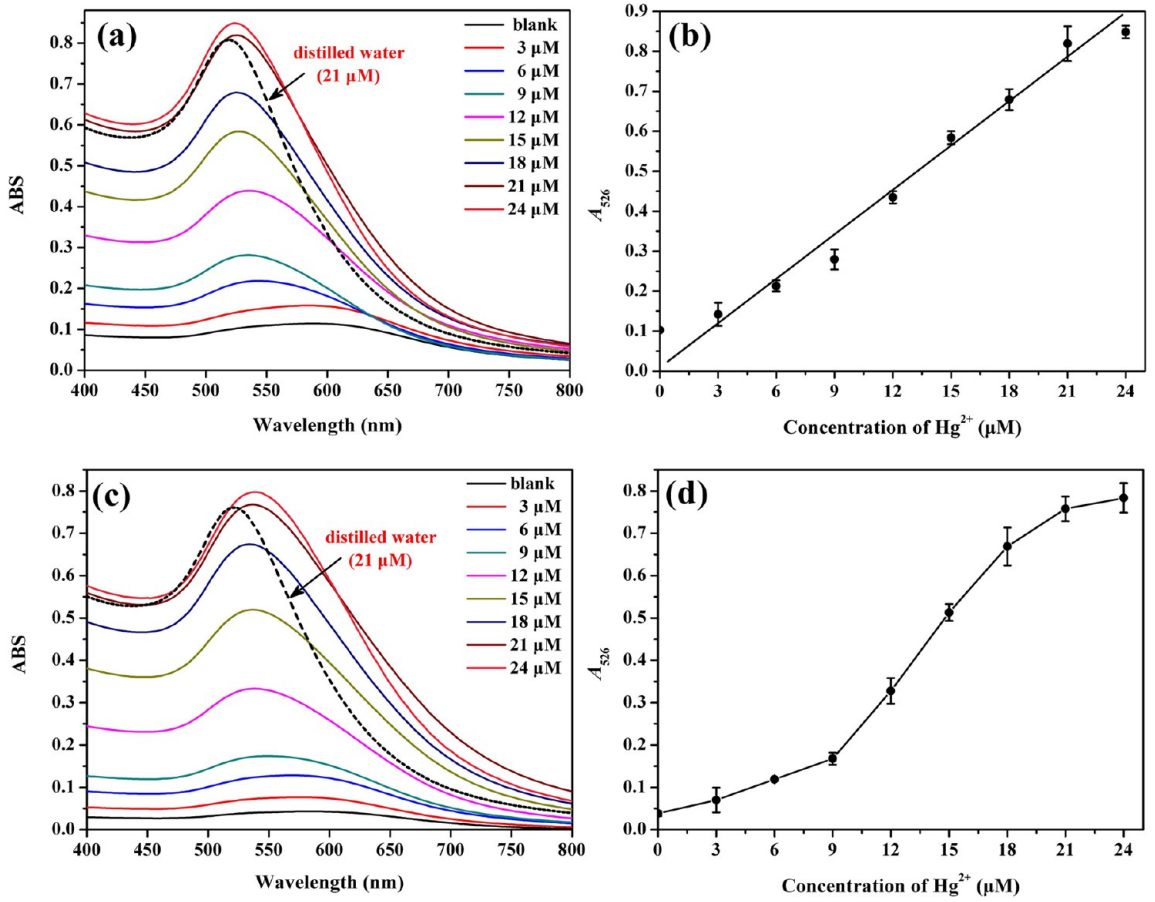

Figure 5. Colorimetric detection of Hg^{2+} in real water samples. UV−vis spectra of Au−CEQC/Cys systems response for the Hg^{2+} concentration in (a) East Lake water and (c) tap water. Plots of A_{526} versus the Hg^{2+} concentration in (b) East Lake water and (d) tap water.

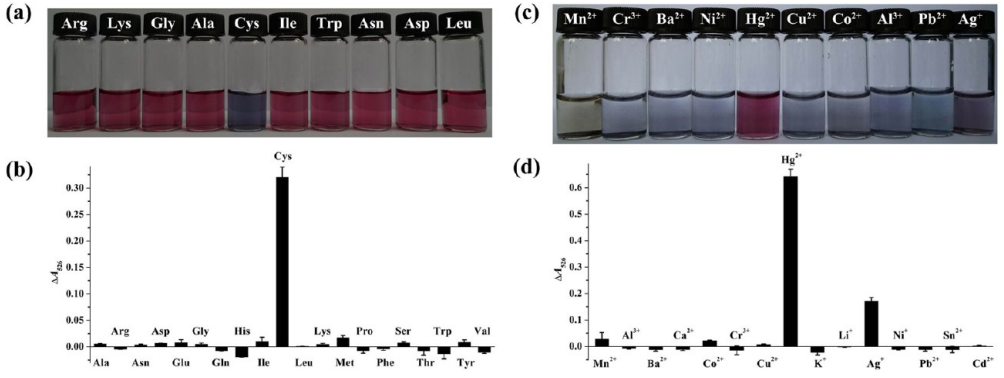

Figure 6. (a) Color change and (b) absorption band at 526 nm for the Au−CEQC solutions in the presence of various amino acids; (c) color change and (d) absorption band at 526 nm for Au−CEQC/Cys systems in the presence of various metallic ions ($c_{\text{amino acid}}$ = 100 μM, c_{cys} = 10 μM, $c_{\text{metallic ions}}$ = 24 μM).

method against different concentrations of biomolecules. It can be seen that the UV−vis spectra exhibited a redshift with decreasing absorbance with increasing DTT concentration (Figure S7a, Supporting Information). The ratio A_{526}/A_{624} was plotted against DTT concentration, and the results exhibited good linearity (Figure S7b, Supporting Information). The LOD for DTT is approximately 23 nM (S_0 = 0.003, S = 0.3993), similar to the LOD for Cys. Thus, this detection assay was also suitable for the quantitative detection of DTT. However, as shown in Figure S7c (Supporting Information), GSH can induce the partially aggregation of Au NPs, but the size of the aggregates do not increase with an increase of GSH concentration, leading to barely any change of the UV−vis spectra of Au−CEQC solutions under relative high GSH concentration. On the other hand, BSA failed to cause any change of the Au−CEQC solution (Figure S7d, Supporting Information), mainly due to its large size, complex structure, and great Coulombic repulsion.[42] Thus, this detection assay was not suitable for the quantitative detection of GSH and BSA.

Sensitivity of Au−CEQC/Cys to Hg^{2+}. It is well known that Hg^{2+} is apt to interact with thiols such as Cys; thus, a rational strategy to probe Hg^{2+} is to combine Cys-functionalized noble

dx.doi.org/10.1021/la3050913 | *Langmuir* 2013, 29, 5085−5092

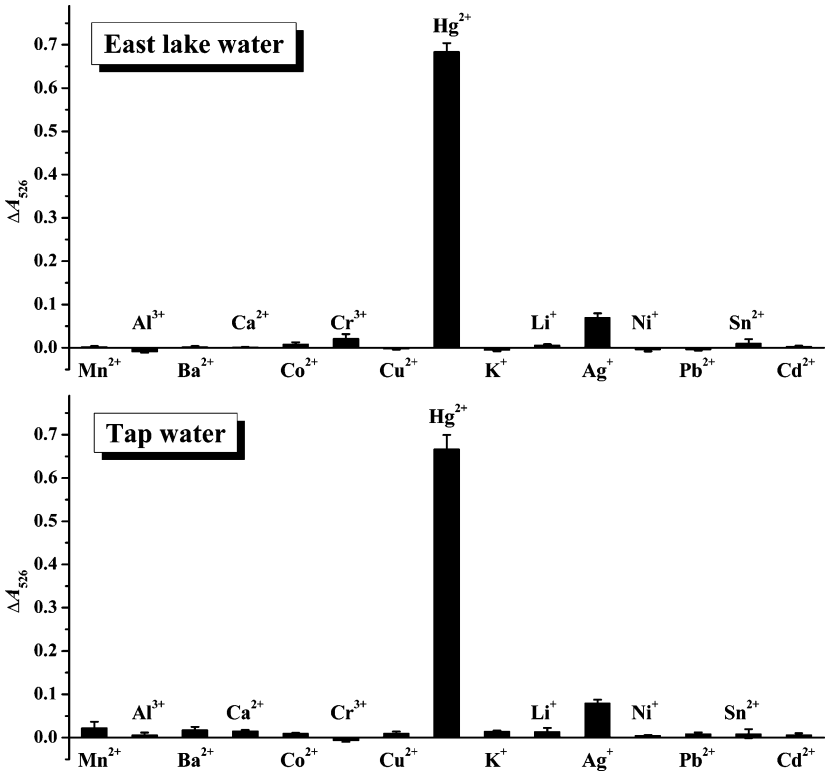

Figure 7. Selective detection of Hg^{2+} in real water samples ($c_{\text{metallic ions}}$ = 24 μM).

metal nanoparticles and Hg^{2+} ions.[43,44] Inspired by this theory, this novel colorimetric assay was further used for the detection of Hg^{2+}. As shown in Figure 3, the UV−vis absorption of Au−CEQC/Cys conjugates is quite weak in the whole range of wavelengths, because Au NPs have been precipitated for the introduction of excess Cys (12.4 μM). When Hg^{2+} ions were added, the color of the solution changed from light blue to red gradually (Figure 3a); meanwhile, the UV−vis absorption at 526 nm increased linearly with increasing Hg^{2+} concentration as shown in Figure 3b,d, because Cys was sequestered from the aggregate through Hg^{2+} complexation, which triggered Au NP redispersion again. This hypothesis was confirmed by the TEM image of the redispersed Au NPs as shown in Figure 3c. The particle size and size distribution of Au NPs changed barely after it underwent an aggregation−redispersion process (Figure S5, Supporting Information). We also used DLS to monitor the change of the Au−CEQC solutions. As shown in Figure 4, the hydrodynamic radius (R_h) distributions of the Au−CEQC solutions changed barely as the pH increased from 5.2 to 11.2 (Figure 4a,b). The peak at about 4 nm ($2R_h$ = 8.0 nm, SD = 1.12 nm) corresponded to the free Au NPs in the solution, which was comparable to that (d = 7.9 nm, SD = 2.30 nm) obtained from TEM. However, the CEQC chains became aggregates, and the signal of free Au NPs disappeared after it underwent an aggregation−redispersion process (Figure 4c), attributing to a small quantity of Cys that connected with Au NPs and CEQC chains. In other words, this competitive process turned on the absorption signal and provided the basis for the colorimetric analysis of Hg^{2+}. The LOD for Hg^{2+} is about 40 nM (S_0 = 0.0004, S = 0.0315), and the sensitivity of the assay could be enhanced by reducing the concentration of the added Cys (Figure S8, Supporting Information).

It was worth noting that Figure 3b was not an inverse behavior of Figure 1b, mainly due to the irreversible dynamic process of aggregation and redispersion of Au NPs. As shown in Scheme 2, Au NPs aggregated, and the size of the aggregates increased gradually with an increase of the Cys concentration. Therefore, the UV−vis spectrum exhibited a redshift with decreasing absorbance. In the Hg^{2+} detection process, Au NPs were released from the huge aggregates (or precipitates) to the solution gradually with the addition of Hg^{2+} ions. Therefore, the change of the spectra in Figure 3b seems like an increase of Au NPs concentration, which is rather different from Figure 1b. Interestingly, this redispersion process was also significantly affected by the pH of the conjugate solution. As shown in Figure S9 (Supporting Information), Hg^{2+} failed to trigger Au NP redispersion when the pH was lower than 10.3. Therefore, an appropriate basic condition (pH = 11.2) was chosen for the whole Hg^{2+} detection experiments. It should be noted that the precipitates of $Hg(OH)_2$ are not formed because Hg^{2+} ions prefer to combine with Cys rather than OH^-.

Application in Real Samples. In order to investigate the practical application of the proposed approach, we applied the method to detect Hg^{2+} in East Lake water and tap water. The real water samples were collected from a freshwater lake in our campus (the East Lake) and the tap water in our lab. Then, a series of samples were prepared by spiking them with standard Hg^{2+} solutions over the range 0−24 μM. The detection of Hg^{2+} in lake water is shown in Figure 5a,b. The absorption at 526 nm increased linearly with an increase of Hg^{2+} concentration in lake water over the range 3−24 μM. The LOD for Hg^{2+} in lake water is about 30 nM (S_0 = 0.0004, S = 0.0391), similar to the results obtained in pure water. However, the response for Hg^{2+} in tap water was different from that in deionized water (Figure 5c,d), presumably due to some organic matter existing in tap water that could react with Hg^{2+} to form an organic complex.[44] In spite of this, this novel colorimetric assay was suitable for the detection of Hg^{2+} in real samples.

dx.doi.org/10.1021/la3050913 | Langmuir 2013, 29, 5085−5092

Selective Detection of Cys and Hg^{2+}. To test the selectivity of Au−CEQC systems, the response of the assay to other essential amino acids (including Ala, Arg, Asn, Asp, Glu, Gly, Gln, His, Ile, Leu, Lys, Met, Pro, Phe, Ser, Trp, Thr, Tyr, and Val; each at 100 μM) was investigated. As shown in Figure 6b, only the Cys system shows a significantly lower absorbance (ΔA_{526} = 0.32) relative to that of the blank. Moreover, this selectivity can be visualized with the naked eye. As shown in Figure 6a, only the Au−CEQC solution containing Cys turned blue, whereas the others were still bright red. The Au−CEQC solution turned to purple after adding a great amount of methionine (Met) (100 μM), due to the existence of the methyl mercapto group in the Met. The new colorimetric assay had quite an extreme selectivity for Cys compared with other amino acids. Meanwhile, as shown in Figure 6c,d, tests of the other eight metal ions (except for Ag^+) showed that this system also performed high selectivity toward Hg^{2+}, which was attributed to the higher stability constants of Hg^{2+}−Cys complexes compared with those of other ions.[45,46] It was worth noting that Ag^+ is a significant interference to this detection system, due to the interaction between Cys and Ag ions. However, due to the formation of AgCl precipitates, this interference was basically eliminated when Hg^{2+} was detected in lake water and tap water (Figure 7).

CONCLUSIONS

CEQC-stabilized Au NPs were prepared, and a facile, cost-effective, and eco-friendly method for the detection of Cys and Hg^{2+} has been developed based on the Au−CEQC systems. The results show that Cys and Hg^{2+} can be detected quickly and accurately with high sensitivity and selectivity against other amino acids and metal ions. CEQC not only plays a role as a capping agent of Au NPs but also affects the aggregate and redispersion process of Au NPs. Compared with other existing analytical methods for Hg^{2+} and Cys detection, this new colorimetric assay has a comparable sensitivity and selectively. Moreover, this method is based on an eco-friendly cellulose derivate and can be easily accomplished by using the naked eye or a common UV−vis spectrophotometer at room temperature, making it particularly useful for the practical applications.

ASSOCIATED CONTENT

Supporting Information

UV−vis spectra; colorimetric detection of the low Cys and Hg^{2+} concentrations; effect of pH and ionic strength of the Au−CEQC solutions on the colorimetric sensing process for Cys; effect of pH of the Au−CEQC/Cys systems on the colorimetric sensing process for Hg^{2+}; size distribution histograms; and a TEM image. This material is available free of charge via the Internet at http://pubs.acs.org.

AUTHOR INFORMATION

Corresponding Author

*Phone: +86-27-87219274; fax: +86-27-68754067; e-mail: zhoujp325@whu.edu.cn.

Notes

The authors declare no competing financial interest.

ACKNOWLEDGMENTS

This work was financially supported by National Natural Science Foundation of China (50973085 and 51273151), Program for New Century Excellent Talents in University (NCET-11-0415), National Basic Research Program of China (973 Program, 2010CB732203), the Open Project of State Key Laboratory Cultivation Base for Nonmetal Composites and Functional Materials, and Fundamental Research Funds for the Central Universities. J.Z. thanks the Japan Society for the Promotion of Science (JSPS) Invitation Fellowship for Research in Japan for the financial support.

REFERENCES

(1) Wood, Z. A.; Schröder, E.; Harris, J. R.; Poole, L. B. Structure, Mechanism and Regulation of Peroxiredoxins. *Trends Biochem. Sci.* **2003**, *28*, 32−40.

(2) Dröge, W.; Holm, E. Role of Cysteine and Glutathione in HIV Infection and Other Diseases Associated with Muscle Wasting and Immunological Dysfunction. *FASEB J.* **1997**, *11*, 1077−1089.

(3) Jacobsen, D. W. Homocysteine and Vitamins in Cardiovascular Disease. *Clin. Chem.* **1998**, *44*, 1833−1843.

(4) Zalups, R. K. Molecular Interactions with Mercury in the Kidney. *Pharmacol. Rev.* **2000**, *52*, 113−143.

(5) Hoyle, I.; Handy, R. D. Dose-Dependent Inorganic Mercury Absorption by Isolated Perfused Intestine of Rainbow Trout, *Oncorhynchus mykiss*, Involves Both Amiloride-Sensitive and Energy-Dependent Pathways. *Aquat. Toxicol.* **2005**, *72*, 147−159.

(6) Wang, W.; Rusin, O.; Xu, X.; Kim, K. K.; Escobedo, J. O.; Fakayode, S. O.; Fletcher, K. A.; Lowry, M.; Schowalter, C. M.; Lawrence, C. M.; Fronczek, F. R.; Warner, I. M.; Strongin, R. M. Detection of Homocysteine and Cysteine. *J. Am. Chem. Soc.* **2005**, *127*, 15949−15958.

(7) Wang, Z.; Lee, J. H.; Lu, Y. Highly Sensitive "Turn-On" Fluorescent Sensor for Hg^{2+} in Aqueous Solution Based on Structure-Switching DNA. *Chem. Commun.* **2008**, *44*, 6005−6007.

(8) Jiang, J.; Liu, W.; Cheng, J.; Yang, L.; Jiang, H.; Bai, D.; Liu, W. A Sensitive Colorimetric and Ratiometric Fluorescent Probe for Mercury Species in Aqueous Solution and Living Cells. *Chem. Commun.* **2012**, *48*, 8371−8373.

(9) Rusin, O.; Luce, N. N. S.; Agbaria, R. A.; Escobedo, J. O.; Jiang, S.; Warner, I. M.; Dawan, F. B.; Lian, K.; Strongin, R. M. Visual Detection of Cysteine and Homocysteine. *J. Am. Chem. Soc.* **2004**, *126*, 438−439.

(10) Lim, S.; Escobedo, J. O.; Lowry, M.; Xu, X.; Strongin, R. Selective Fluorescence Detection of Cysteine and *N*-Terminal Cysteine Peptide Residues. *Chem. Commun.* **2010**, *46*, 5707−5709.

(11) Spătaru, N.; Sarada, B. V.; Popa, E.; Tryk, D. A.; Fujishima, A. Voltammetric Determination of L-Cysteine at Conductive Diamond Electrodes. *Anal. Chem.* **2001**, *73*, 514−519.

(12) Liu, S.; Nie, H.; Jiang, J.; Shen, G.; Yu, R. Electrochemical Sensor for Mercury(II) Based on Conformational Switch Mediated by Interstrand Cooperative Coordination. *Anal. Chem.* **2009**, *81*, 5724−5730.

(13) Lu, C.; Zu, Y.; Yam, V. W. W. Nonionic Surfactant-Capped Gold Nanoparticles as Postcolumn Reagents for High-Performance Liquid Chromatography Assay of Low-Molecular-Mass Biothiols. *J. Chromatogr., A* **2007**, *1163*, 328−332.

(14) Chen, H.; Chen, J.; Jin, X.; Wei, D. Determination of Trace Mercury Species by High Performance Liquid Chromatography−Inductively Coupled Plasma Mass Spectrometry after Cloud Point Extraction. *J. Hazard. Mater.* **2009**, *172*, 1282−1287.

(15) Li, Y.; Chen, C.; Li, B.; Sun, J.; Wang, J.; Gao, Y.; Zhao, Y.; Chai, Z. Elimination Efficiency of Different Reagents for the Memory Effect of Mercury Using ICP-MS. *J. Anal. At. Spectrom.* **2006**, *21*, 94−96.

(16) Zhang, J.; Xu, X.; Yuan, Y.; Yang, C.; Yang, X. A Cu@Au Nanoparticle-Based Colorimetric Competition Assay for the Detection of Sulfide Anion and Cysteine. *ACS Appl. Mater. Interfaces* **2011**, *3*, 2928−2931.

(17) Xue, X.; Wang, F.; Liu, X. One-Step, Room Temperature, Colorimetric Detection of Mercury (Hg^{2+}) Using DNA Nanoparticle Conjugates. *J. Am. Chem. Soc.* **2008**, *130*, 3244−3245.

(18) Yu, C.; Tseng, W. Colorimetric Detection of Mercury(II) in a High-Salinity Solution Using Gold Nanoparticles Capped with 3-Mercaptopropionate Acid and Adenosine Monophosphate. *Langmuir* **2008**, *24*, 12717−12722.

(19) Lee, J. S.; Ulmann, P. A.; Han, M. S.; Mirkin, C. A. A DNA−Gold Nanoparticle-Based Colorimetric Competition Assay for the Detection of Cysteine. *Nano Lett.* **2008**, *8*, 529−533.
(20) Srivastava, S.; Frankamp, B. L.; Rotello, V. M. Controlled Plasmon Resonance of Gold Nanoparticles Self-Assembled with PAMAM Dendrimers. *Chem. Mater.* **2005**, *17*, 487−490.
(21) Nam, J.; Won, N.; Jin, H.; Chung, H.; Kim, S. pH-Induced Aggregation of Gold Nanoparticles for Photothermal Cancer Therapy. *J. Am. Chem. Soc.* **2009**, *131*, 13639−13645.
(22) Polavarapu, L.; Xu, Q. Water-Soluble Conjugated Polymer-Induced Self-Assembly of Gold Nanoparticles and Its Application to SERS. *Langmuir* **2008**, *24*, 10608−10611.
(23) Chen, Y.; Yu, C.; Cheng, T.; Tseng, W. Colorimetric Detection of Lysozyme Based on Electrostatic Interaction with Human Serum Albumin-Modified Gold Nanoparticles. *Langmuir* **2008**, *24*, 3654−3660.
(24) Saha, K.; Agasti, S. S.; Kim, C.; Li, X.; Rotello, V. M. Gold Nanoparticles in Chemical and Biological Sensing. *Chem. Rev.* **2012**, *112*, 2739−2779.
(25) Liu, D.; Qu, W.; Chen, W.; Zhang, W.; Wang, Z.; Jiang, X. Highly Sensitive, Colorimetric Detection of Mercury(II) in Aqueous Media by Quaternary Ammonium Group-Capped Gold Nanoparticles at Room Temperature. *Anal. Chem.* **2010**, *82*, 9606−9610.
(26) Li, T.; Dong, S.; Wang, E. Label-Free Colorimetric Detection of Aqueous Mercury Ion (Hg^{2+}) Using Hg^{2+}-Modulated G-Quadruplex-Based DNAzymes. *Anal. Chem.* **2009**, *81*, 2144−2149.
(27) Klemm, D.; Heublein, B.; Fink, H. P.; Bohn, A. Cellulose: Fascinating Biopolymer and Sustainable Raw Material. *Angew. Chem., Int. Ed.* **2005**, *44*, 3358−3393.
(28) Song, Y.; Sun, Y.; Zhang, X.; Zhou, J.; Zhang, L. Homogeneous Quaternization of Cellulose in NaOH/Urea Aqueous Solutions as Gene Carriers. *Biomacromolecules* **2008**, *9*, 2259−2264.
(29) Song, Y.; Wang, H.; Zeng, X.; Sun, Y.; Zhang, X.; Zhou, J.; Zhang, L. Effect of Molecular Weight and Degree of Substitution of Quaternized Cellulose on the Efficiency of Gene Transfection. *Bioconjugate Chem.* **2010**, *21*, 1271−1279.
(30) Song, Y.; Zhou, J.; Li, Q.; Guo, Y.; Zhang, L. Preparation and Characterization of Novel Quaternized Cellulose Nanoparticles as Protein Carriers. *Macromol. Biosci.* **2009**, *9*, 857−863.
(31) You, J.; Zhou, J.; Li, Q.; Zhang, L. Rheological Study of Physical Cross-Linked Quaternized Cellulose Hydrogels Induced by *β*-Glycerophosphate. *Langmuir* **2012**, *28*, 4965−4973.
(32) Song, Y.; Gan, W.; Li, Q.; Guo, Y.; Zhou, J.; Zhang, L. Homogenous Modification of Cellulose with Acrylamide in NaOH/Urea Aqueous Solutions. *Carbohydr. Polym.* **2011**, *86*, 171−176.
(33) Liu, J. C.; Anand, M.; Roberts, C. B. Synthesis and Extraction of *β*-D-Glucose-Stabilized Au Nanoparticles Processed into Low-Defect, Wide-Area Thin Films And Ordered Arrays Using CO_2-Expanded Liquids. *Langmuir* **2006**, *22*, 3964−3971.
(34) Laudenslager, M. J.; Schiffman, J. D.; Schauer, C. L. Carboxymethyl Chitosan as a Matrix Material for Platinum, Gold, and Silver Nanoparticles. *Biomacromolecules* **2008**, *9*, 2682−2685.
(35) Guo, Y.; Wang, Z.; Qu, W.; Shao, H.; Jiang, X. Colorimetric Detection of Mercury, Lead and Copper Ions Simultaneously Using Protein-Functionalized Gold Nanoparticles. *Biosens. Bioelectron.* **2011**, *26*, 4064−4069.
(36) Kim, Y. R.; Mahajan, R. K.; Kim, J. S.; Kim, H. Highly Sensitive Gold Nanoparticle-Based Colorimetric Sensing of Mercury(II) through Simple Ligand Exchange Reaction in Aqueous Media. *ACS Appl. Mater. Inter.* **2010**, *2*, 292−295.
(37) Sun, Z.; Ni, W.; Yang, Z.; Kou, X.; Li, L.; Wang, J. pH-Controlled Reversible Assembly and Disassembly of Gold Nanorods. *Small* **2008**, *4*, 1287−1292.
(38) Aryal, S.; K.C., R. B.; Bhattarai, N.; Kim, C. K.; Kim, H. Y. Study of Electrolyte Induced Aggregation of Gold Nanoparticles Capped by Amino Acids. *J. Colloid Interface Sci.* **2006**, *299*, 191−197.
(39) Mocanua, A.; Cernicab, I.; Tomoaiac, G.; Bobosa, L. D.; Horovitz, O.; Tomoaia-Cotisel, M. Self-Assembly Characteristics of Gold Nanoparticles in the Presence of Cysteine. *Colloids Surf., A* **2009**, *338*, 93−101.
(40) Zhang, S.; Kou, X.; Yang, Z.; Shi, Q.; Stucky, G. D.; Sun, L.; Wang, J.; Yan, C. Nanonecklaces Assembled from Gold Rods, Spheres, and Bipyramids. *Chem. Commun.* **2007**, 1816−1818.
(41) Guan, Z.; Li, S.; Cheng, P. B. S.; Zhou, N.; Gao, N.; Xu, Q. Band-Selective Coupling-Induced Enhancement of Two-Photon Photoluminescence in Gold Nanocubes and Its Application as Turnon Fluorescent Probes for Cysteine and Glutathione. *ACS Appl. Mater. Interfaces* **2012**, *4*, 5711−5716.
(42) Hu, B.; Zhao, Y.; Zhu, H.; Yu, S. Selective Chromogenic Detection of Thiol-Containing Biomolecules Using Carbonaceous Nanospheres Loaded with Silver Nanoparticles as Carrier. *ACS Nano* **2011**, *5*, 3166−3171.
(43) Jiang, C.; Guan, Z.; Lim, S. Y. R.; Polavarapu, L.; Xu, Q. Two-Photon Ratiometric Sensing of Hg^{2+} by Using Cysteine Functionalized Ag Nanoparticles. *Nanoscale* **2011**, *3*, 3316−3320.
(44) Lou, T.; Chen, Z.; Wang, Y.; Chen, L. Blue-to-Red Colorimetric Sensing Strategy for Hg^{2+} and Ag^{+} via Redox-Regulated Surface Chemistry of Gold Nanoparticles. *ACS Appl. Mater. Inter.* **2011**, *3*, 1568−1573.
(45) Lee, J.-S.; Han, M. S.; Mirkin, C. A. Colorimetric Detection of Mercuric Ion (Hg^{2+}) in Aqueous Media Using DNA-Functionalized Gold Nanoparticles. *Angew. Chem., Int. Ed.* **2007**, *46*, 4093−4096.
(46) Miyake, Y.; Togashi, H.; Tashiro, M.; Yamaguchi, H.; Oda, S.; Kudo, M.; Tanaka, Y.; Kondo, Y.; Sawa, R.; Fujimoto, T.; Machinami, T.; Ono, A. $Mercury^{II}$-Mediated Formation of Thymine−Hg^{II}−Thymine Base Pairs in DNA Duplexes. *J. Am. Chem. Soc.* **2006**, *128*, 2172−2173.